IEEE Photonics Journal
An IEEE Photonics Society Publication

Nanowire Grid Reflecting Polarizers for Ultraviolet Applications

Volume 12, Number 6, December 2020

Zhuan Zhao, *Student Member, IEEE*
Alain Jody Corso
Maria Guglielmina Pelizzo

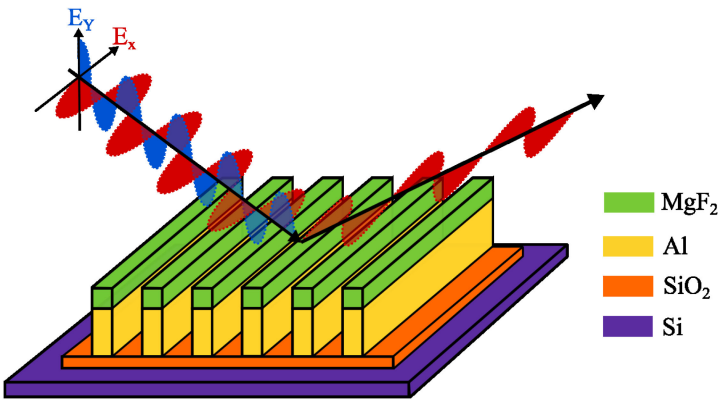

DOI: 10.1109/JPHOT.2020.3031341

IEEE photonics SOCIETY
IEEE

Nanowire Grid Reflecting Polarizers for Ultraviolet Applications

Zhuan Zhao,[1] ***Student Member, IEEE***, **Alain Jody Corso**,[1,2] **and Maria Guglielmina Pelizzo**[1,2]

[1]Department of Information Engineering, University of Padova, Padova 35131, Italy
[2]National Research Council of Italy, Institute for Photonics and Nanotechnologies e Padova, Padova 35131, Italy

DOI:10.1109/JPHOT.2020.3031341

Manuscript received August 27, 2020; revised September 29, 2020; accepted October 12, 2020. Date of publication October 15, 2020; date of current version December 15, 2020. Corresponding author: Zhuan Zhao (e-mail: zhaozhuan2008@gmail.com).
This article has supplementary downloadable material available at https://ieeexplore.ieee.org, provided by the authors.

Abstract: Polarimetry in the far ultraviolet (FUV) is a powerful tool in many applications such as UV/EUV ellipsometry, characterization and control of the beam polarization status in large scale facilities and solar physics. FUV polarizers are among the most difficult components to manufacture, mainly due to the lack of dichroic and transparent materials in this spectral range. Although many different solutions for their fabrication have been investigated in the last decades, surprisingly, the use of Wire Grid Polarizers (WGPs) is still poorly investigated in this spectral region. In this work, two different concepts of WGPs have been designed and optimized for the FUV range: one is based on absorptive nano-wires on top of an highly reflective substrate, and the second one is based on highly reflective nano-wires on top of an absorptive substrate. Different wires' shapes have been considered and relative structures optimized at a target wavelength of 121.6 nm. Two very promising solutions have been selected, which exhibit a polarization degree over 99.9% and a TE-reflectance over 0.2. Their sensitivity to the wires' dimension parameters have been investigated to assess their feasibility.

Index Terms: TE-reflectance, wire grid polarizers, far ultraviolet, optimization, polarization.

1. Introduction

Polarimetry in the far-ultraviolet (FUV) and extreme-ultraviolet (EUV) wavelength range is a technique that has recently grown in importance in many fields of modern science, including FUV/EUV ellipsometry [1], characterization and control of the beam polarization in synchrotrons [2]–[4] and free-electron laser sources [2], [5]–[8], and solar physics [9], [10]. A very interesting application in which the FUV polarimetry finds large employment is the measurement of solar magnetic field vector in the solar corona made via the Hanle effect [11] by using observation from space. The bright lines in which the Hanle effect is particularly evident are the H_I Ly-α at 121.6 nm, the H_I Ly-β at 102.5 nm, the H_I Ly-γ at 97.2 nm and the O_{VI} doublet at 103.2 nm and 103.8 nm [12]. Considering these target lines, many examples of space missions with FUV polarimeters and spectro-polarimeters have been proposed, such as CLASP 1 [13], [14], SolmeX [15] and COMPASS [16]. Nevertheless, the realization of such kind of instruments is still challenging,

basically due to the technical difficulties encountered in the development of the main optical components.

Optical polarizers are among the most critical components in FUV polarimetric instrumentation mainly due to the small number of low-absorbent materials available in this spectral range. MgF_2 is perhaps the most used and studied material for its fair transparency at $\lambda > 115$ nm (i.e., the MgF_2 cutting-edge). Below this limit, LiF is the only other material with low absorption for $\lambda > 102.5$ nm, but its hygroscopicity highly degrades the transmittance just after a moderate humidity exposure [17]. Thus, in principle, among the lines previously listed only the H_I Ly-α can be manipulated with a polarizer working in transmission. For example, the birefringence of the MgF_2 bulk crystal makes the realization of transmissive polarizing beam-splitter feasible, like the Rochon or Wollaston prisms. In particular, MgF_2 Wollaston prisms were proposed for astronomical polarimetry in the FUV [18] even if the relatively small deviation angles achievable ($\simeq 20^\circ$) require the adoption of an instrumental geometry characterized by large optical paths and, consequently, small throughput. Wire-grid polarizers (WGPs), which consist of periodic arrays of nano-metallic wires placed on a transmissive substrate, are an effective alternative to polarizing prisms. The anisotropic behavior given by the nano-metallic wires performs a high absorption of the radiation along a precise direction without affecting the transmittance of the orthogonal one. Although the WGPs are largely employed in the near ultraviolet ($\lambda > 193$ nm), visible and infrared [19], the extension to the FUV range, and in particular to the H_I Ly-α line, is currently a challenge of the nanotechnology [20].

As an alternative, polarizers based on optical coatings can be used when polarization is required at one specific wavelength, although they are usually characterized by a low transmittance. For instance, a fair transmissive linear polarizer tuned around 121.6 nm was obtained by realizing a stack of 3-4 bilayers of Al/MgF_2 [21]. Moreover, by exploiting the high reflectance of aluminum in this spectral range, a polarizing beam-splitter able to simultaneously select one polarization component by reflection and the perpendicular component by transmission has been fabricated [22]. The idea of adopting polarizing films working in reflection may give additional benefits. Firstly, at wavelengths longer than the MgF_2 cutting-edge the Al-protected mirrors show a reflectance up to 90% [23], which offers a good basis for the development of high efficiency polarizers [21], [24]–[26]. Moreover, materials having good reflection properties also below the MgF_2 cutting-edge are available, enabling the possibility of developing polarizers for wavelengths shorter than 115 nm [27], [28].

Polarizing mirrors, which can reflect the desired polarization component with high efficiency, need to work with large incidence angles, sometimes greater than 70° [21], entailing instruments having polarization analyzer with grazing geometries and small throughput. In most cases, the configuration is based on the combination of various reflectance components. For example, the adoption of polarization-sensitive studies such as spin-polarized photoelectron spectroscopy and spectroscopic ellipsometry in synchrotron facilities has driven the research of new technological solutions [29], [30]. An example of a configuration based on a gold triple-reflection was reported in [31], which can achieve a polarization between 90% and 96% at the energy range from 2 eV to 40 eV. In addition, a triple- reflected gold polarizer for testing VUV ELIps capabilities in the VUV spectral region from 30 eV to 45 eV has been developed [32]. Nevertheless, compact reflective polarizers which can achieve extremely high polarization in the spectral energy below 10 eV are still difficult to realize.

A different approach, which is still uninvestigated so far in the FUV range, consists of using reflective-WGPs [33]. By placing either reflective nano-wires on an absorptive substrate or absorptive nano-wires on a reflective substrate it is possible to achieve the anisotropic behavior in which a polarization component is efficiently reflected/absorbed whereas the orthogonal one is efficiently absorbed/reflected. Furthermore, since this method is not strictly connected to the interference process used in the thin polarizing films, the reflective-WGPs can act as a polarizer at different wavelengths. Such solution can provide very flexible and compact polarizers, which can be optimized for different incidence angles and that can work on a wide spectral range.

In this paper, the theoretical design of reflective-WGPs has been investigated considering as target wavelength the H_I Ly-α line at 121.6 nm. Different materials and shapes for the nano-wires

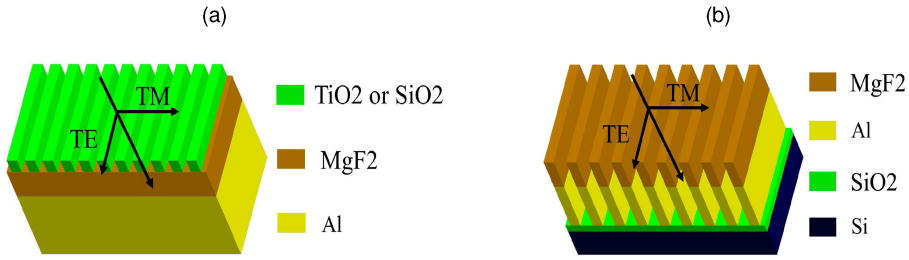

Fig. 1. The two concept of reflective-WGP investigated: (a) model based on absorptive nano-wires, (b) model based on reflective nano-wires.

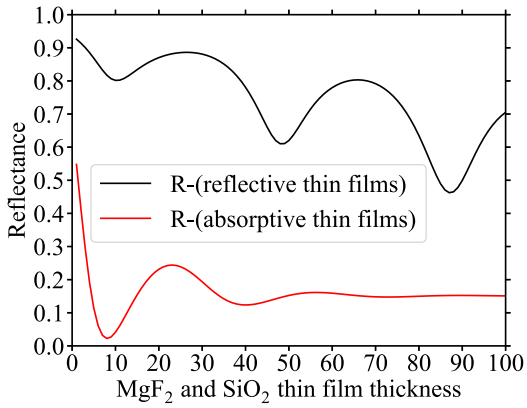

Fig. 2. The reflectance at $\lambda = 121.6$ nm of a MgF_2 layer on a Al substrate (black solid curve) and of a SiO_2 layer on a Si substrate (red solid curve). All the simulation has been performed considering a working angle of 45° and the optical constants available in the references reported in Table 1.

have been explored in order to identify the most promising structures. Optimization of the structures have been carried out and most promising solutions selected and discussed in view of their fabrication.

2. Design and Modelling

Two different reflective-WGP concepts for the realization of a polarizer optimized at $\lambda = 121.6$ nm have been studied (Fig. 1). As shown, the electric field of the impinging beam is split into two components, the transverse electric (TE), which is oriented along the wires, and the transverse magnetic (TM), which is perpendicular to the wires. The first reflective-WGP concept is based on a high-reflective mirror optimized for a target wavelength (i.e., $\lambda = 121.6$ nm) on top of which absorptive nano-wires are exploited for removing the TM-component. The high reflectance is achieved by using an optically-thick Al layer (i.e., about 150 nm) over-coated by an optimized MgF_2 layer for preventing oxidation [23]. The optimization of the MgF_2 thickness was carried out using IMD software for an incidence angle of 45°, which is a typical incidence angle useful for folding mirrors in optical systems. The results are reported in Fig. 2, where the reflectance at the working angle has been plotted versus the MgF_2 thickness (solid black curve). A thickness of 65 nm has been chosen because it produces a constructive interference and at the same time, ensures a good level of protection.

The nano-wires placed on top of the reflective bi-layers structure need to be fabricated using a material with low reflection and relative high absorption around the target wavelength. Such conditions suggests a family of materials whose refractive index has a real part n between 1

TABLE 1
Optical Constants At λ =121.6 nm of the Materials Considered in This Work

Material	n	k	Reference
Al	0.0423	1.1404	[34]
MgF_2	1.7047	0.0180	[35]
SiO_2	1.9644	0.5793	[36]
TiO_2	1.1222	0.9157	[37]
Si	0.295	1.32	[38]

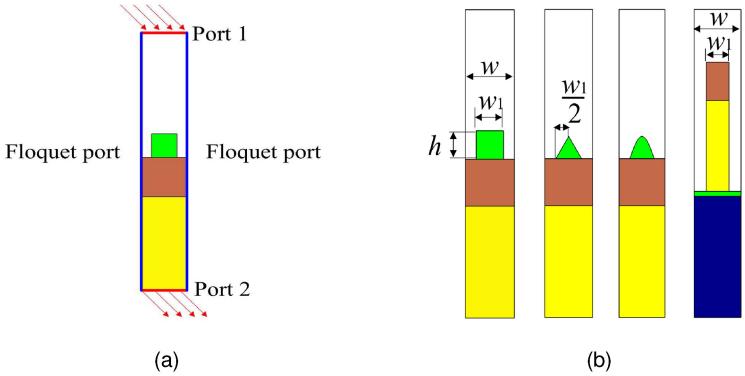

Fig. 3. The 2-D boundary model used in the structures simulation. (a) The ports used in the model for imposing the boundary conditions required in the electric field computation. (b) The wires' shapes investigated in this work.

and 2 and a imaginary part *k* between 0.5 and 1. Metals show a quite good reflectance in the FUV since they usually have a real part *n* close to zero and the imaginary part *k* greater than 1. On the other hand, fluorides are characterized by a high transparency due to the low value of the imaginary part of refractive index. Oxides, instead, are the materials which better meet the requirements for refractive index; among these, TiO_2 and SiO_2 have been selected as nano-wires' material candidates. The optical constants of the materials considered in this work are reported in Table 1 with the related references.

The second concept is based on high reflective nano-wires placed on a non-reflective substrate (Fig. 1(b)), which acts the polarization selection by efficiently reflecting only the TE-component of the impinging electric field. In this case, efficient reflective nano-wires can be obtained starting from the same Al/MgF_2 mirror, which is etched in order to obtain the wires grating structure. Simulations used Si wafer as substrate which, however, typically shows a marked reflectance at λ =121.6 nm (i.e., >50%). In order to further reduce this value, a SiO_2 anti-reflection layer is added between the substrate and the reflective nano-wires. In Fig. 2, the solid red line is the reflectance at λ =121.6 nm of a SiO_2 layer deposited on a Si wafer as function of layer thickness, the working angle considered is still 45°. The thickness of 8 nm was selected because it allows to reduce the reflectance at a value $\simeq$ 3%.

The simulations of these structures at $\lambda = 121.6$ nm have been carried out in Wave Optics Module of COMSOL Multiphysics software by using the 2D boundary mode analysis. The solutions are based on finite element method (FEM) and the electric field is computed in all materials by solving via the following equation

$$\nabla \times (\mu_r^{-1} \nabla \times \vec{E}) - k_0 \left(\epsilon_r - \frac{j\sigma}{\omega \epsilon_0} \right) \vec{E} = 0 \tag{1}$$

where $k_0 = \omega \sqrt{\mu_0 \epsilon_0}$ is the wavenumber, μ_r and ϵ_r are the relative magnetic and dielectric permettivities of the medium, ϵ_0 is the vacuum electric permettivity and σ is the media conductivity. The 2D structure simulated is depicted in Fig. 3(a). The impinging beam excites the structure from

TABLE 2
Sweeping Ranges Used for the Optimization of the WGP Structures

WGP topology	Sweeping range
Absorptive wires	h: [1, 200] nm, w_1: [20, 200] nm, w: [w_1, 200] nm
Reflective wires	w_1: [20, 200] nm, w: [w_1, 200] nm

TABLE 3
Optimized Parameters

Absorptive WGPs					
Optimization label	Wires' shape	Wires' material	Wires' parameters	R_{TE}	P
Design A	rectangle	TiO_2	h = 38 nm, w_1 = 38 nm, w = 68 nm	0.21407	99.970%
Design B	rectangle	SiO_2	h = 115 nm, w_1 = 110 nm, w = 114 nm	0.23700	99.857%
Design C	triangle	TiO_2	h = 48 nm, w_1 = 69 nm, w = 71 nm	0.25234	99.998%
Design D	triangle	SiO_2	h = 64 nm, w_1 = 137 nm, w =146 nm	0.09093	99.993%
Design E	sine	TiO_2	h = 96 nm, w_1 = 68 nm, w = 121 nm	0.12225	99.999%
Design F	sine	SiO_2	h = 89 nm, w_1 = 94 nm, w =141 nm	0.07771	99.580%
Reflective WGPs					
Design G	rectangle	Al/MgF_2	w_1 = 39 nm, w = 80 nm	0.30149	99.991%

the upper port (i.e., port 1, on-top of the vacuum media) inducing a back-reflected wave that is evaluated by the port itself. The bottom port (i.e., port 2) acts as output port, implementing the bulk boundary condition for the substrate material. To reproduce the periodicity condition in the horizontal dimension, Floquet ports are used for the boundary conditions of the left and right sides. In our specific case the incident beam is linearly polarized and impinges on the structure at the nominal angle of 45°.

In the case of structures based on highly absorbing wires, three different shapes for such nanowires were considered (see Fig. 3(b)): the square, the isosceles triangle and a cosine. All these shapes can be easily described by using only three parameters: the pitch, w, the wires' width, w_1 and the wires' height, h. On the other hand, for the structure based on high-reflective nonowires, only the square shape was investigated; in this case, the wires are unequivocally defined by the parameters w and w_1, because the wires' height is pre-determined by the high reflectance condition. The performance of all structures were evaluated by considering the value of reflectance for the TE-component and the polarization degree defined as

$$P = \frac{R_{TE} - R_{TM}}{R_{TE} + R_{TM}} \tag{2}$$

where R_{TE} and R_{TM} are the reflectance for the TE and TM component, respectively. The maxima of the polarization degree function P for each structure was found by sweeping the parameters w, w_1 and, when necessary, h into the value ranges reported in Table 2. In this way, all local maxima were considered in the optimization process allowing for each the evaluation of the absolute TE-reflectance. Only the solutions having a nominal polarization degree P more than 99.5% and a R_{TE} more than 0.2 were taken into further consideration.

3. Results and Discussion

All the structures obtained from the optimization process are summarized in Table 3. Some of these show poor performance in terms of R_{TE} or P, making them unacceptable for the purpose of the present study. For example, the structures with cosine-shaped absorptive wires (i.e., design

E and F in Table 3) as well as the SiO_2 triangle-shaped absorptive wires (i.e., design D) are not able to achieve the minimum requirements of TE-reflectance, although some of them give a very high polarization degree. The structure with SiO_2 rectangle-shaped absorptive wires (i.e., design B) is also discarded: despite this solution achieves the requirements in both the reflectance and polarization degree, it shows a ratio $\frac{w_1}{w} \simeq 0.96$ making this structure very challenging for the available manufacturing technologies.

Designs A, C and G are the most promising structures in term of performance. In particular, all these structures have good performance in term of polarization factor *P*, although the designs based on absorptive nano-wires (i.e., A, and C) give a lower TE-reflectance than those based on reflective nano-wires (design G). In principle, in the structures based on absorptive nano-wires, the TE-component is efficiently reflected by the substrate and, with a lesser extent, from the wires themselves. In contrast, since the TM-component is perpendicular to the absorptive wires, the radiation propagates through the grid but the high absorption of the nano-wires strongly reduces the final reflectance. For a fixed material and wire shape, the attenuation of the TM-component (i.e., and then of the polarization factor *P*) is highly dependent on the grid pitch and wires' height. However, as all the designs presented in this work are characterized by a w/λ ratio between 0.55–1.2, the gaps between the absorbent nano-wires have a size-scale such as to induce a lossy propagation towards the reflective substrate also for the TE wave. Consequently, the substrate contribution to the TE-reflectance dramatically degrades with the nano-wires volume fraction ($\propto w_1/w$) and their height. Thus, the overall efficiency of such structures is decreased by the non-negligible effects of losses affecting the TE-component of the radiation. In WGPs based on reflective wires, the TE-reflectance is only given by the nano-wires. The transparency of the MgF_2 at these wavelengths guarantees that the TE-radiation is well-reflected at the interface between MgF_2 and Al, with an additional small improvement given by the constructive interference of the MgF_2 layer. On the other hand, the TM-wave is transmitted through the metal wires grid because magnetic fields do not cause vibrations in the conducting electrons of the metallic grid. Although the TM-component undergoes some losses during the transmission, the TM-component is efficiently attenuated from the anti-reflective properties of the substrate. Therefore, the overall efficiency expected from reflective-wires structures is greater than that given by structures based on absorptive-wires.

The determination of the best solution also requires the evaluation of the sensitivity performance with respect to the values of the parameters w, w_1 and *h* obtained during the optimization process. Currently, WGPs with a pitch $\geq$ 100 nm can be easily manufactured with very high precision by using nano-imprinting lithography [39]–[42]. However, the fabrication of repeatable and precise WGPs with a pitch $\leq$ 100 nm is still a challenge, [43]–[47] mainly due to the high technical complexity and cost associated to the use of the techniques available in the industry so far, such as EUV lithography, laser writing, e-beam direct writing, or holographic interference in a production environment. Fortunately, many new methods have been proposed and are still under investigation in order to fabricate such periodical nanometric-pitched structures. For example, Liu *et al.* [48] fabricated a 38 nm half-pitch grating over large areas by using combined immersion holography and low-temperature atomic spacer lithography. Pelletier *et al.* [49] fabricated a 16.5 nm half-pitch wire grid in a cheap way, through the use of a self-assembling diblock copolymer mask whereas Fan *et al.* [50] reported a patterning of line/spaces with an HP of 6 nm by using HSQ photoresist via EUV IL. All these results make the manufacturing of our WGPs feasible.

The sensitivity was investigated by sweeping w and w_1 parameters in the range $\pm$20% from the nominal value with a step of 1 nm. Since the height of nano-wires is easily to be guaranteed in the model deposition processes, only a sweep of $\pm$ 1 nm from the nominal value was considered for the structures based on absorptive wires. The results obtained are reported in Fig. 4. The evaluation of the robustness of a structure is based on the determination of the range within each parameter can vary to maintain a variation of the polarization degree *P* less than 2% with respect to the nominal value and the TE-reflectance higher than 20%. The acceptable ranges of the parameters w and w_1 computed for Design A, C and E are reported in Table 4.

Among the absorptive WGPs, Design A shows the highest acceptable range for both w and w_1 since the performance in term of polarization degree and TE-reflectance remain acceptable if the

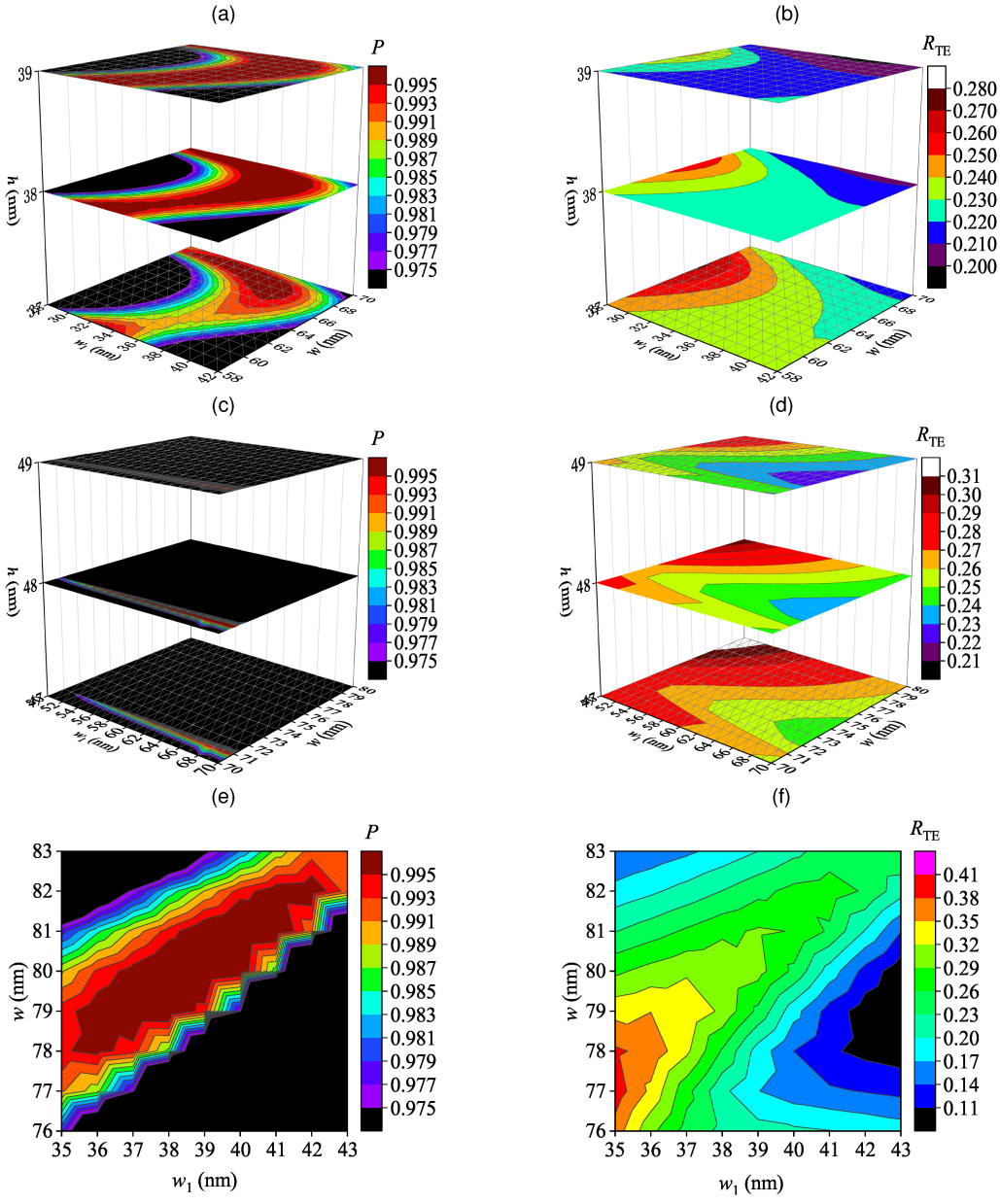

Fig. 4. Sensitivity analysis for the Design A, C and G. (a) and (b): the polarization degree and the TE reflectance versus free parameters of Design A; (c) and (d): the polarization degree and the TE reflectance versus free parameters of Design C; (e) and (f): the polarization degree and the TE reflectance versus free parameters of Design G.

TABLE 4

Acceptable Range for w and w_1 Which Ensure a Drop of the Polarization Degree *P* Less Than 2% With Respect to the Nominal Value and the TE-Reflectance Higher Than 20%

–	w		w_1	
Structure	nominal value	acceptable range	nominal value	acceptable range
Design A	68 nm	62 - 70 nm	38 nm	33 - 40 nm
Design C	71 nm	70 - 72 nm	69 nm	65 - 70 nm
Design G	80 nm	79 - 82 nm	39 nm	37 - 40 nm

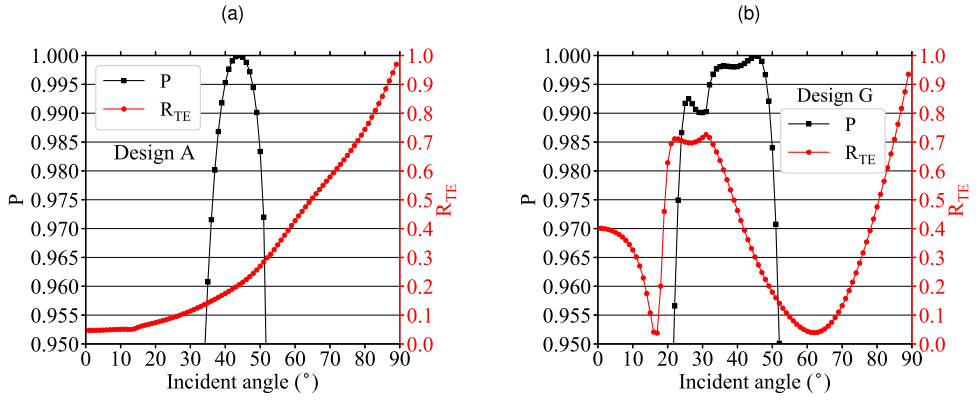

Fig. 5. (a) Polarization angular behavior of Design A, (b) Polarization angular behavior of Design G.

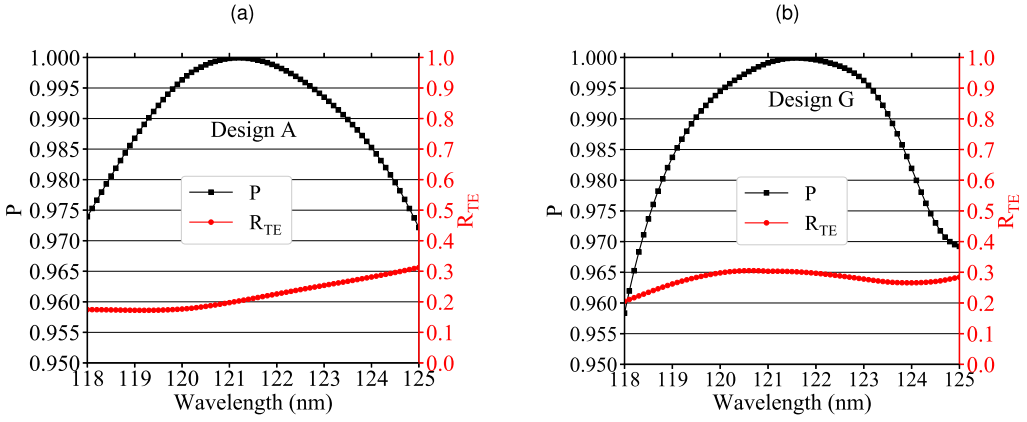

Fig. 6. (a) Wavelength behavior of Design A, (b) Wavelength behavior of Design G.

period w and the width w_1 fall in the range of 62–70 nm and 33–40 nm, respectively. In contrast, the polarization degree given by Design C is very sensitive to the structure periodicity, requiring a precision within 1 nm for the wires' period (see Table 4), which turns out to be very challenging for the current manufacturing technology. Finally, the reflective WGP of Design G shows an acceptable range of 79–82 nm for w and 37–40 nm for w_1: despite these limits are more stringent than Design A, this structure is still feasible and worthy of attention considering its high TE-reflectance.

Further features which may be of interest in many applications are the variation of the performance with respect to the incidence angle and the wavelength. Fig. 5 reports the performance of the Design A and G as function of the incidence angle, still considering the nominal wavelength at 121.6 nm. Applying the criteria adopted for the nominal evaluation, the Design A is the most critical as the structure shows acceptable performance for incidence angles only range from 44° up to 50°. On the other hand, the performance of Design G are maintained over a large range of angles from 24°, where $R_{TE} = 0.705$, up to 49°.

Similarly, Fig. 6 reports the performance change as function of the wavelength. In this case, both structures show a similar behaviour, although the Design G is better in term of TE-reflectance. In fact for the Design A the performance is acceptable in the wavelength range between 121.2 nm and 124.8 nm, while for the Design G the range increases from 118.6 nm up to 124.3 nm. The undesired losses which affect the TE-component in absorptive WGPs are highly dependent on the incident wavelength and angle, making this structure more sensitive to these parameters. Anyway, considering both angular and spectral performance, all those structures show valuable results although Design G is a little bit superior.

4. Conclusion

In this paper, the design of wire grid polarizers (WGP) intended for working at 121.6 nm wavelength (H Ly-α) have been investigated. Two different approaches were considered, one based on absorptive nano-wires on a Al/MgF_2 high-reflective mirror and the other one based on reflective nano-wires placed on a Si non-reflective substrate. The nominal performance required for considering acceptable WGP solutions was a reflectance of 0.2 at the target wavelength and a polarization degree *P* of 99.9%.

Two promising structures were selected throughout the optimization process, both are composed of squared nano-wires. The first one, named Design A, is based on TiO_2 absorptive wires having a height of 38 nm, a width of 38 nm and placed with a pitch of 68 nm; simulations given a TE-reflectance of 21.4% and a polarization degree *P* of 99.97% for this structure. Instead, the second structure, named Design G, is based on reflective wires obtained with the Al(150 nm)/MgF_2(65 nm) bi-layer with a width of 39 nm and a pitch of 80 nm; with this structure, a TE-reflectance of 30.1% and a polarization degree *P* of 99.99% can be achieved.

The robustness of the performance with respect to the width and pitch variation were investigated for the two promising structures. This evaluation is based on the determination of the range within each parameter can vary to maintain a variation of the polarization degree *P* less than 2% with respect to the nominal value and the TE-reflectance higher than 20%. For Design A, the performance remain acceptable when the pitch and width in the range of 62–70 nm and 33–40 nm whereas for the Design G in the range 79–82 nm and 37–40 nm, respectively. In conclusion, despite the Design G has a narrower ranges of robustness, this structure is the preferable candidate since it shows the best performance. This choice is further strengthened by comparing the angular and spectral ranges within which the performance remain acceptable: 44° up to 50° and 121.2 nm and 124.8 nm for Design A against 24° to 49° and 118.6 nm up to 124.3 nm for Design G.

References

[1] T. Saito *et al.*, "Vacuum ultraviolet ellipsometer using inclined detector as analyzer to measure stokes parameters and optical constants – with results for aln optical constants," *Thin Solid Films*, vol. 571, pp. 517–521, 2014, 6th International Conference on Spectroscopic Ellipsometry (ICSE-VI). [Online]. Available: https://www.sciencedirect.com/science/article/pii/S004060901400265X

[2] B. Watts, L. Thomsen, and P. Dastoor, "A simple polarimeter for quantifying synchrotron polarization," *J. Electron Spectrosc. Related Phenom.*, vol. 151, no. 3, pp. 208–214, 2006. [Online]. Available: https://www.sciencedirect.com/science/article/pii/S0368204805005244

[3] C. von Korff Schmising *et al.*, "Generating circularly polarized radiation in the extreme ultraviolet spectral range at the free-electron laser flash," *Rev. Sci. Instrum.*, vol. 88, no. 5, 2017, Art. no. 053903.

[4] T. Harada and T. Watanabe, "Reflectance measurement of EUV mirrors with s-and p-polarized light using polarization control units," in *Proc. Int. Conf. Extreme Ultraviolet Lithography 2018*, vol. 10809. International Society for Optics and Photonics, 2018, Paper 108091T.

[5] E. Roussel *et al.*, "Roussel2017," *Photon.*, vol. 4, no. 2, 2017. [Online]. Available: https://www.mdpi.com/2304-6732/4/2/29

[6] L. Nahon and C. Alcaraz, "Su5: A calibrated variable-polarization synchrotron radiation beam line in the vacuum-ultraviolet range," *Appl Opt*, vol. 43, no. 5, pp. 1024–1037, 2004.

[7] P. Finetti *et al.*, "Polarization measurement of free electron laser pulses in the vuv generated by the variable polarization source fermi," in *Proc. SPIE*, vol. 9210, 2014, Art. no. 92100K.

[8] E. Allaria *et al.*, "Control of the polarization of a vacuum-ultraviolet, high-gain, free-electron laser," *Physical Review X*, vol. 4, no. 4, 2014, Art. no. 041040.

[9] P.-M. Robitaille and D. Rabounski, "Polarized light from the sun: Unification of the corona and analysis of the second solar spectrum–further implications of a liquid metallic hydrogen solar model," *Progress*, vol. 11, 2015.

[10] N. Narukage *et al.*, "High-reflectivity coatings for a vacuum ultraviolet spectropolarimeter," *Solar Phys.*, vol. 292, no. 3, 2017.

[11] S. Fineschi, R. B. Hoover, J. M. Fontenla, and A. B. C. W. II, "Polarimetry of extreme ultraviolet lines in solar astronomy," *Opt. Eng.*, vol. 30, no. 8, pp. 1161–1168, 1991. [Online]. Available: https://doi.org/10.1117/12.55922

[12] S. Fineschi, "Space-based Instrumentation for Magnetic Field Studies of Solar and Stellar Atmospheres," in *Magnetic Fields Across the Hertzsprung-Russell Diagram*, (Astronomical Society of the Pacific Conference Series), G. Mathys, S. K. Solanki, and D. T. Wickramasinghe, Eds., vol. 248, Jan. 2001.

[13] R. Kano *et al.*, "Chromospheric lyman-alpha spectro-polarimeter (clasp)," in *Proc. SPIE*, vol. 8443, 2012, Art. no. 84434F.

[14] N. Narukage *et al.*, "Chromospheric layer spectropolarimeter (clasp2)," in *Proc. SPIE*, vol. 9905, 2016, Art. no. 990508.

[15] H. Peter *et al.*, "Solar magnetism explorer (solmex)," *Exp. Astron.*, vol. 33, no. 2-3, pp. 271–303, 2012.
[16] W. Ley, E. Plescher, A. Scholz, and J. Piepenbrock, "Compass-1 picosatellite project," in *Proc. 6th IAA Symp. Small Satellites for Earth Observation. Berlin, Germany*, 2007.
[17] S. Wilbrandt, O. Stenzel, H. Nakamura, D. Wulff-Molder, A. Duparré, and N. Kaiser, "Protected and enhanced aluminum mirrors for the vuv," *Appl. Opt.*, vol. 53, no. 4, pp. A125–A130, Feb. 2014. [Online]. Available: https://ao.osa.org/abstract.cfm?URI=ao-53-4-A125
[18] C. Neiner *et al.*, and The UVMag consortium, "Uvmag: stellar formation, evolution, structure and environment with space uv and visible spectropolarimetry," *Astrophysics and Space Sci.*, vol. 354, no. 1, pp. 215–227, Nov. 2014. [Online]. Available: https://doi.org/10.1007/s10509-014-2050-4
[19] T. Siefke *et al.*, "Materials pushing the application limits of wire grid polarizers further into the deep ultraviolet spectral range," *Adv. Opt. Mater.*, vol. 4, no. 11, pp. 1780–1786, 2016.
[20] M. Pancrazzi *et al.*, "Updates on the pencil project," *Nuovo Cimento C Geophys. Space Physics C*, vol. 42, 2019.
[21] J. I. Larruquert *et al.*, "Reflective and transmissive broadband coating polarizers in a spectral range centered at 121.6 nm," *J. Opt.*, vol. 16, no. 12, 2014, Art. no. 125713.
[22] J. I. Larruquert *et al.*, "Polarizers tuned at key far-uv spectral lines for space instrumentation," in *Proc. SPIE*, vol. 10235, 2017, Art. no. 102350K.
[23] L. V. R. D. Marcos *et al.*, "Optimization of mgf2-deposition temperature for far uv al mirrors," *Opt. Express*, vol. 26, no. 7, pp. 9363–9372, Apr. 2018. [Online]. Available: https://www.opticsexpress.org/abstract.cfm?URI=oe-26-7-9363
[24] J. I. Larruquert *et al.*, "Polarizers for a spectral range centered at 121.6 nm operating by reflectance or by transmittance," in *Proc. SPIE*, vol. 9510, 2015, Art. no. 951008.
[25] F. Bridou, M. Cuniot-Ponsard, J.-M. Desvignes, A. Gottwald, U. Kroth, and M. Richter, "Polarizing and non-polarizing mirrors for the hydrogen lyman-α radiation at 121.6 nm," *Appl. Phys. A*, vol. 102, no. 3, pp. 641–649, 2011.
[26] J. Kim, M. Zukic, M. M. Wilson, and D. G. Torr, "Design and fabrication of a reflection far-ultraviolet polarizer and retarder," in *Proc. SPIE*, 1994, vol. 2010, pp. 93–103.
[27] L. V. R. D. Marcos *et al.*, "Lyman-β narrowband coatings with strong lyman-α rejection," *Opt. Express*, vol. 26, no. 19, pp. 25 166–25 177, Sep. 2018. [Online]. Available: https://www.opticsexpress.org/abstract.cfm?URI=oe-26-19-25166
[28] J. I. Larruquert, L. V. R. de Marcos, J. A. Méndez, P. J. Martin, and A. Bendavid, "High reflectance ta-c coatings in the extreme ultraviolet," *Opt. Express*, vol. 21, no. 23, pp. 27 537–27 549, Nov. 2013. [Online]. Available: https://www.opticsexpress.org/abstract.cfm?URI=oe-21-23-27537
[29] M. Yang, "Yang2007," *J. Optics A: Pure Appl. Opt.*, vol. 9, 2007. [Online]. Available: https://iopscience.iop.org/article/10.1088/1464-4258/9/10/025/meta
[30] G. Black *et al.*, "Euv stokes reflection polarimeter using gold coated mirrors for use up to 150 ev photon energy," in *Proc. SPIE*, 2019, vol. 11109, Art. no. 111090G.
[31] M. Neumann *et al.*, "A synchrotron-radiation-based variable angle ellipsometer for the visible to vacuum ultraviolet spectral range," *Rev. Sci. Instrum.*, vol. 85, no. 5, 2014, Art. no. 055117.
[32] S. Espinoza *et al.*, "Characterization of the high harmonics source for the vuv ellipsometer at eli beamlines," *J. Vac. Sci. Technol. B, Nanotechnol. Microelectronics: Mater., Process., Meas., Phenomena*, vol. 38, no. 2, 2020, Art. no. 024005.
[33] J. M. Papalia, D. H. Adamson, P. M. Chaikin, and R. A. Register, "Silicon nanowire polarizers for far ultraviolet (sub-200 nm) applications: Modeling and fabrication," *J. Appl. Phys.*, vol. 107, no. 8, 2010, Art. no. 084305.
[34] D. Smith, E. Shiles, and M. Inokuti, "The optical properties of metallic aluminum," in *Handbook of Optical Constants of Solids*, E. D. Palik, Ed. New York, NY, USA: Academic, 1997, pp. 369–406. [Online]. Available: https://www.sciencedirect.com/science/article/pii/B9780125444156500169
[35] L. V. R. de Marcos, J. I. Larruquert, J. A. Méndez, and J. A. Aznárez, "Self-consistent optical constants of mgf2, laf3, and cef3 films," *Opt. Mater. Express*, vol. 7, no. 3, pp. 989–1006, Mar. 2017. [Online]. Available: https://www.osapublishing.org/ome/abstract.cfm?URI=ome-7-3-989
[36] L. V. Rodríguez-de Marcos, J. I. Larruquert, J. A. Méndez, and J. A. Aznárez, "Self-consistent optical constants of sio 2 and ta 2 o 5 films," *Opt. Mater. Express*, vol. 6, no. 11, pp. 3622–3637, 2016.
[37] D. Franta, D. Nečas, and I. Ohlídal, "Universal dispersion model for characterization of optical thin films over a wide spectral range: application to hafnia," *Appl. Opt.*, vol. 54, no. 31, pp. 9108–9119, Nov. 2015. [Online]. Available: https://ao.osa.org/abstract.cfm?URI=ao-54-31-9108
[38] D. P. Edward and I. Palik, "Handbook of optical constants of solids," 1985.
[39] J. J. Wang *et al.*, "30-nm-wide aluminum nanowire grid for ultrahigh contrast and transmittance polarizers made by uv-nanoimprint lithography," *Appl. Phys. Lett.*, vol. 89, no. 14, 2006, Art. no. 141105.
[40] J. J. Wang, F. Walters, X. Liu, P. Sciortino, and X. Deng, "High-performance, large area, deep ultraviolet to infrared polarizers based on 40 nm line/78 nm space nanowire grids," *Appl. Phys. Lett.*, vol. 90, no. 6, 2007, Art. no. 061104.
[41] F. Meng, G. Luo, I. Maximov, L. Montelius, J. Chu, and H. Xu, "Fabrication and characterization of bilayer metal wire-grid polarizer using nanoimprint lithography on flexible plastic substrate," *Microelectronic Eng.*, vol. 88, no. 10, pp. 3108–3112, 2011.
[42] E. E. Scime, E. H. Anderson, D. J. McComas, and M. L. Schattenburg, "Extreme-ultraviolet polarization and filtering with gold transmission gratings," *Appl. Opt.*, vol. 34, no. 4, pp. 648–654, 1995.
[43] S.-W. Ahn *et al.*, "Fabrication of a 50 nm half-pitch wire grid polarizer using nanoimprint lithography," *Nanotechnol.*, vol. 16, no. 9, 2005, Art. no. 1874.
[44] R. Kunz, M. Rothschild, and M. Yeung, "Large-area patterning of 50 nm structures on flexible substrates using near-field 193 nm radiation," *J. Vac. Sci. Technol. B: Microelectron. Nanometer Struct. Process., Meas., Phenom.*, vol. 21, no. 1, pp. 78–81, 2003.
[45] D. J. Resnick *et al.*, "Imprint lithography for integrated circuit fabrication," *J. Vac. Sci. Technol. B Microelectron. Nanometer Struct.*, vol. 21, no. 21, pp. 2624–2631, 2003.

[46] C. Pentico, E. Gardner, D. Hansen, and R. Perkins, "52.4: New, high performance, durable polarizers for projection displays," in *Proc. SID Symp. Dig. Tech. Papers*, vol. 32, no. 1. Wiley Online Library, 2001, pp. 1287–1289.
[47] F. Hua *et al.*, "Polymer imprint lithography with molecular-scale resolution," *Nano Lett.*, vol. 4, no. 12, pp. 2467–2471, 2004.
[48] X. Liu *et al.*, "Large area, 38 nm half-pitch grating fabrication by using atomic spacer lithography from aluminum wire grids," *Nano Lett.*, vol. 6, no. 12, pp. 2723–2727, 2006.
[49] V. Pelletier, K. Asakawa, M. Wu, D. H. Adamson, R. A. Register, and P. M. Chaikin, "Aluminum nanowire polarizing grids: Fabrication and analysis," *Appl. Phys. Lett.*, vol. 88, no. 21, 2006, Art. no. 211114.
[50] D. Fan and Y. Ekinci, "Photolithography reaches 6 nm half-pitch using extreme ultraviolet light," *J. Micro/ Nanolithography, MEMS, MOEMS*, vol. 15, no. 3, 2016, Art. no. 033505.